Triangular formation control using range measurements:

An application to marine robotic vehicles

Jorge M. Soares [*,**] **A. Pedro Aguiar** [*] **António M. Pascoal** [*]
Marco Gallieri [***]

[*] *Laboratory of Robotics and Systems in Engineering and Science,*
Instituto Superior Técnico, Technical University of Lisbon,
Av. Rovisco Pais, 1049-001 Lisboa, Portugal
(emails: {jsoares,pedro,antonio}@isr.ist.utl.pt)
[**] *School of Architecture, Civil and Environmental Engineering,*
École Polytechnique Fédérale de Lausanne (EPFL),
CH-1015 Lausanne, Switzerland
[***] *Control Group, Engineering Department, Sidney Sussex College,*
University of Cambridge, CB21PZ Cambridge, UK
(email: mg574@eng.cam.ac.uk)

Abstract: This paper addresses the problem of maintaining an autonomous robotic vehicle in a moving triangular formation by regulating its position with respect to two leader vehicles. The robotic vehicle has no a priori knowledge of the path described by the leaders and its goal is to follow them by constantly regulating the inter-vehicle distances to a desired fixed value, using range-only measurements. To solve this station keeping problem, we propose a control strategy that estimates the formation speed and heading from the ranges obtained to the two leading vehicles, and uses simple feedback laws for speed and heading commands to drive suitably defined common and differential errors to zero. For straight-line motion, we provide guaranteed conditions under which the proposed control strategy achieves local convergence of the distance errors to zero. We also indicate how our design procedure can be extended to full dynamic models of marine robotic vehicles equipped with inner loops for yaw and speed control. Simulation results using realistic models are described and discussed.

Keywords: Autonomous Vehicles; Marine Systems; Control Laws; Lyapunov Stability; Formation Control; Station Keeping; Triangular Formations.

1. INTRODUCTION

Spawned by the advent of small embedded processors and sensors and miniaturized actuators, there is widespread interest in the development of fleets of autonomous marine vehicles with the potential to drastically improve the means available for ocean exploration and exploitation. In fact, the use of multiple autonomous robotic vehicles acting cooperatively has been steadily gaining more acceptance as a way to increase the performance, reliability, and effectiveness of automated systems at sea. The scientific and commercial missions envisioned are manifold and include marine habitat mapping, geophysical surveying, and adaptive ocean sampling, to name but a few.

In some of the most challenging missions (e.g. marine habitat mapping in complex 3D environments) it is fundamental that a number of vehicles carrying different sensor suites and navigation equipment maneuver in formation at close range, cooperating towards the acquisition of environmental data. From a technical standpoint, meeting this objective requires that the vehicles be equipped with advanced systems for networked navigation and control.

In a representative mission scenario, one of the vehicles (known as the anchor) is equipped with an advanced sensor suite for absolute geo-referencing so as to follow a desired path or to maneuver along arbitrary trajectories in response to episodic events. It is up to the remaining vehicles to join and keep a desired formation with the anchor, effectively moving along at the same speed. In these circumstances, it is crucial that vehicles be parsimonious with the information that they exchange over the inter-vehicle communication system in order to reach formation. A solution that is both elegant and cost-effective is to do formation control by relying on inter-vehicle range measurements only. The latter can be obtained by equipping the vehicles with acoustic ranging devices.

The general problem of cooperative motion control has been the subject of much research over the past few years, as reflected in a sizable body of publications in the area of networked control systems and robotics. Some of this work falls in the scope of cooperative path following, where a group of vehicles is required to maneuver along pre-specified paths while keeping a desire formation pattern

(absolute formation control). See Ghabcheloo et al. (2009) for work along these lines with applications in the marine field. In the work reported, each vehicle is required to know its absolute position and those of the neighboring vehicles. This is in contrast with the work in Cao et al. (2007), where the objective is not to do absolute formation control but relative formation control instead. In this situation, each vehicle is only required to know the position of some of the neighbors in its own reference frame. From a practical point of view, however, this still poses formidable challenges when the vehicles move underwater.

Related work can be found in Desai et al. (1998, 2001) on the so-called leader-follower formation control problem for a formation graph with an arbitrary number of vehicles. In the work cited, two approaches were proposed using either range-bearing or range-range control, depending on the available sensors. In both approaches, knowledge of the leader motion was assumed. A strikingly different strategy is described in Cao and Morse (2007, 2008), where a solution is proposed for a 4-vehicle station keeping problem, using exclusively range measurements. The authors formulate a decentralized control policy using switched adaptive control. The vehicle dynamics correspond to single integrators in 2D.

More recently, in Cao et al. (2011) the authors advance algorithms to coordinate a formation of mobile agents when the agents can only measure the distances to their respective neighbors. To control the shape of the formation, the solution proposed requires that subsets of non-neighbor agents cyclically localize the relative positions of their respective neighbor agents while these are held stationary, and then move to reduce the value of a cost function; the latter is nonnegative and assumes the zero value precisely when the formation has correct distances. Again, it is assumed that the mobile agents can be described by kinematic points.

Motivated by the above considerations, and as a contribution towards the solution of the general formation keeping problem, this paper addresses the simplified problem of maintaining an autonomous vehicle in a moving triangular formation with respect to two leader vehicles that move at equal velocities, with a fixed distance between them. The vehicle has no a priori knowledge of the path described by the leaders and its goal is to follow them by constantly regulating the inter-vehicle distances to desired values, using range-only measurements. One real-world situation that matches this scenario is that of a group composed of two autonomous surface craft (leader vehicles) equipped with GPS and radio communications and one autonomous underwater vehicle (AUV) lacking both. In this case, the follower AUV computes its distance to each of the surface craft by measuring the time-of-flight of acoustic pulses.

In the present paper we adopt a kinematic model for the follower AUV that is not a simple double integrator. Instead, the model is written in terms of the vehicle's speed and heading. We propose a control strategy that estimates the formation speed and heading from the ranges obtained to the two leading vehicles, and uses simple feedback laws for speed and heading commands to drive suitably defined common and differential errors to zero. For straight-line motion, we provide guaranteed conditions under which the proposed control strategy achieves local convergence
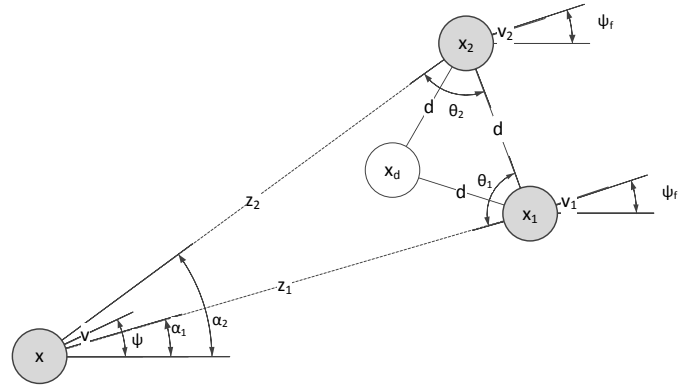

Fig. 2.1. Triangular formation control

of the distance errors to zero. As an intermediate step needed to apply the algorithms derived in the real world, we indicate how our design procedure can be extended to a full dynamic model of marine robotic vehicles equipped with inner loops for yaw and speed control. Simulation results using a realistic model of an existing marine vehicle and more complex paths are described and discussed.

The paper is organized as follows: in Section 2, we present an overview of the problem at hand and introduce some basic notation; in Section 3 we derive the error dynamics and the control laws for linear velocity and heading, present the formation heading estimation method, and outline the stability proofs; in Section 4 we introduce the dynamic model for a representative marine vehicle and describe an extension of our work to such a scenario; in Section 5 we show some simulation results using this model. Finally, in Section 6 we present our conclusions and possible future directions for this research.

2. PROBLEM STATEMENT

The control problem studied in this paper is depicted in Fig. 2.1, which shows two leading vehicles and a follower. The objective is for the trailing vehicle (vehicle 0) to follow the other two in a triangular formation, at the same distance d from each of them. In the figure, x should converge to the desired position x_d. The control signals are the linear velocity v and the heading ψ, and the kinematic model of the follower is given by

$$\dot{x} = \begin{bmatrix} v \cos \psi \\ v \sin \psi \end{bmatrix}, \qquad (2.1)$$

where $x \in \mathbb{R}^2$ denotes its Cartesian position. The leader vehicles (1 and 2) move at a distance d from each other, according to

$$\dot{x}_i = \begin{bmatrix} v_i \cos \psi_i \\ v_i \sin \psi_i \end{bmatrix}, \quad i = 1, 2 \qquad (2.2)$$

where $(v_1 + v_2)/2 = v_f$ is the formation speed. In what follows we assume that $v_1 = v_2$ and $\psi_1 = \psi_2$. We further assume that the total velocity vector of each leading vehicle is always perpendicular to the line segment that joins them. Formally, we define the formation orientation, denoted ψ_f, as $\psi_1 = \psi_2 = \psi_f$. We assume that ψ_f is unknown to vehicle 0. Note that there exists a symmetric solution to the problem, with the desired position x_d mirrored in relation to the segment defined by $x_2 \, x_1$. We designate the solution shown in Fig. 2.1 by *following motion*, and the mirrored

solution by *leading motion*. In the remainder of this paper, we will only deal with the case of following motion.

The trailing vehicle can measure its distance to each leader, given by $z_i = \|x - x_i\|$. From the range measurements, we define the common and differential mode errors

$$\epsilon = \frac{e_1 + e_2}{2} = \frac{z_1 + z_2}{2} - d$$

$$\delta = e_2 - e_1 = z_2 - z_1,$$

with $e_i = z_i - d, i = 1, 2$. The control problem consist of deriving feedback laws for v and ψ to drive ϵ and δ to zero or, equivalently, to drive x to x_d.

3. CONTROL DESIGN

This section describes the strategy adopted to regulate the motion of the trailing vehicle. We assume its starting position is behind the two leading vehicles, relative to their movement direction. Two separate controllers are designed, one to regulate the vehicle speed and one for the vehicle heading. Each controller is responsible for stabilizing a different error measure, the common mode error and the differential mode error, respectively.

3.1 Error dynamics

From the definition of z_i, it follows that

$$\dot{z}_i = \frac{(x_i - x)^T (\dot{x}_i - \dot{x})}{z_i}.$$

Inserting (2.1) and (2.2) in the above equation yields

$$\dot{z}_i = v_i \cos(\alpha_i - \psi_f) - v \cos(\alpha_i - \psi), \qquad (3.1)$$

where α_i is the angle of the unit vector

$$\begin{bmatrix} \cos \alpha_i \\ \sin \alpha_i \end{bmatrix} = \frac{x_i - x}{z_i}.$$

Simple computations show that the relations between α_i and the interior angles of the triangle θ_i in Fig. 2.1 are given by

$$\alpha_1 = \theta_1 + \psi_f - \frac{\pi}{2}$$

$$\alpha_2 = -\theta_2 + \psi_f + \frac{\pi}{2}.$$

The law of cosines allows us to obtain the following expressions for θ_i

$$\theta_1 = \arccos\left(\frac{z_1^2 + d^2 - z_2^2}{2\,d\,z_1} \right)$$

$$\theta_2 = \arccos\left(\frac{z_2^2 + d^2 - z_1^2}{2\,d\,z_2} \right).$$

Although the control strategy holds potential to be applied to other types of trajectories, as shown later, the results presented in the next sections assume the simpler case of straight line constant-speed motion for the two leading vehicles. In this case, $v_1 = v_2 = v_f$, and the error dynamics for ϵ and δ become

$$\dot{\epsilon} = \cos \beta \left(v_f \cos \varphi - v \cos(\varphi + \tilde{\psi}) \right) \qquad (3.2)$$

$$\dot{\delta} = 2 \sin \beta \left(v_f \sin \varphi - v \sin(\varphi + \tilde{\psi}) \right), \qquad (3.3)$$

where

$$\beta = \frac{\alpha_1 - \alpha_2}{2} = \frac{\theta_1 + \theta_2}{2} - \frac{\pi}{2}$$

$$\varphi = \frac{\alpha_1 + \alpha_2}{2} - \psi_f = \frac{\theta_1 - \theta_2}{2},$$

and $\tilde{\psi} = \psi_f - \psi$ is the heading error. Notice that θ_1 and θ_2 are interior angles of the same triangle, and therefore $0 < \theta_1, \theta_2, \theta_1 + \theta_2 < \pi$, $\beta \in (-\frac{\pi}{2}, 0)$ and $\varphi \in (-\frac{\pi}{2}, \frac{\pi}{2})$.

3.2 Speed controller

We propose the following speed controller to regulate the common mode error ϵ to zero:

$$v = K_p^s \epsilon + K_i \int_0^t \epsilon \, d\tau, \qquad (3.4)$$

where $K_p^s > 0$ and $K_i > 0$ are the proportional and integral gains, respectively. The rationale for the proposed control law can be explained by observing that when the leader vehicles are describing a straight-line trajectory with constant speed v_f, $\psi = \psi_f$ and $\delta = 0$ (i.e., x_0 is placed on the perpendicular bisector of the $x_1 x_2$ line segment), the dynamics of ϵ in (3.2) reduce to

$$\dot{\epsilon} = \cos \beta (v_f - v). \qquad (3.5)$$

In this case, and since $\cos \beta > 0$, a control law $v = v_f + K_p^s \epsilon$, $K_p^s > 0$ would exponentially stabilize the origin $\epsilon = 0$, provided β does not converge to $-\frac{\pi}{2}$. As v_f is unknown, we include an integral term to learn it.

Theorem 1. Consider the overall system consisting of two leader vehicles (1 and 2) undergoing a straight-line motion with constant but unknown velocity $v_f > 0$. Suppose that $\psi = \psi_f$ and that vehicle 0 lies in a neighborhood of the perpendicular bisector of $x_1 x_2$, in a following position. Then, for a sufficiently small integral gain K_i (with respect to K_p^s), the control law (3.4) locally exponentially stabilizes ϵ to the origin $\epsilon = 0$.

Proof. (Theorem 1) Defining $\dot{\xi} = K_i \epsilon$, we get $v = \xi + K_p^s \epsilon$. Introducing the error term $\tilde{v} = \xi - v_f$ yields $\dot{\tilde{v}} = \dot{\xi} - \dot{v}_f = K_i \epsilon$. Using (3.5) we obtain

$$\begin{bmatrix} \dot{\epsilon} \\ \dot{\tilde{v}} \end{bmatrix} = \begin{bmatrix} -K_p^s \cos \beta & -\cos \beta \\ K_i & 0 \end{bmatrix} \begin{bmatrix} \epsilon \\ \tilde{v} \end{bmatrix}. \qquad (3.6)$$

Linearizing system (3.6) at the equilibrium point corresponding to the equilateral triangular position ($\epsilon = 0$, $\delta = 0$, $\beta^* = \frac{\pi}{6}$), it follows that the eigenvalues of the state matrix are negative for $K_i < \frac{\sqrt{3}}{8} K_p^s$, thus proving the theorem. $\square$

3.3 Heading controller

For the heading controller we propose the following control law that uses the differential mode error δ:

$$\psi = \hat{\psi}_f + \gamma(K_p^h \delta), \qquad (3.7)$$

where $K_p^h > 0$, $\hat{\psi}_f$ denotes an estimate of the formation heading ψ_f, and γ is any function such that $\sin(\gamma(ay))y > 0, \forall a > 0$. An example is the saturation function $\gamma(y) = \frac{\pi}{2} \text{sat}(y)$. For a constant speed straight-line motion with $\epsilon = 0$ and $v = v_1 = v_2$, (3.3) yields

$$\dot{\delta} = 2v_f \sin \beta \left(\sin \varphi - \sin(\varphi + \tilde{\psi}) \right). \qquad (3.8)$$

The use of γ is motivated by the fact that the control law appears within a sine argument.

Theorem 2. Consider the overall system consisting of two leader vehicles (1 and 2) describing a straight-line motion with constant velocity $v_f > 0$. Suppose that $v = v_f$, ψ_f is known and vehicle 0 lies in a trailing position, and

that there exist positive constants $D > \mu > 0$ such that $d + \mu < z_1 + z_2 < D$. Then, the control law (3.7) stabilizes δ to the origin $\delta = 0$.

The next result is instrumental in proving Theorem 2.

Proposition 1. Suppose that $z_1 + z_2 > d$. Then, the signal of $\sin \varphi$ is the same as the signal of δ, i.e., $\sin(\varphi)\delta > 0$.

Proof. (Proposition 1) For $\delta = 0$, $z_1 = z_2$ and the terms in φ cancel out. For $\delta > 0$ and $z_1 + z_2 > d$, we have

$$\frac{z_2^2 + d^2 - z_1^2}{2\,d\,z_2} > \frac{z_1^2 + d^2 - z_2^2}{2\,d\,z_1}$$
$$\implies \theta_1 > \theta_2$$
$$\implies \varphi > 0.$$

An analogous argument can be derived for $\delta < 0$. $\qquad\square$

Remark 1. The condition $z_1 + z_2 \geq d$ is a physical constraint, since vehicles 1 and 2 are separated by a distance d. When $z_1 + z_2 = d$, vehicle 0 is located along the line segment $x_1 x_2$. This does not fit the definition of a following motion.

Proof. (Theorem 2) Define the candidate Lyapunov function

$$V_h = \frac{1}{2}\delta^2 > 0.$$

Using (3.8) and the control law (3.7) we obtain

$$\dot{V}_h = 2v_f \sin \beta \left(\sin \varphi - \sin \varphi \cos \tilde{\psi} - \cos \varphi \sin \tilde{\psi} \right) \delta$$
$$= 2v_f \sin \beta$$
$$\qquad \left(\left(1 - \cos(\gamma(K_p^h \delta)) \right) \sin \varphi + \cos \varphi \sin(\gamma(K_p^h \delta)) \right) \delta$$
$$< 0.$$

The last condition stems from the fact that $\sin(\varphi)\delta > 0$, $\sin(\gamma(K_p^h \delta))\delta > 0$ and, because $d + \mu < z_1 + z_2 < D, D > \mu > 0$, there exist positive constants $c_i, i = 1, 2, 3$ such that $\sin \beta < -c_1$, $\cos \beta > c_2$ and $\cos \varphi > c_3$. $\qquad\square$

3.4 Stability of the overall system

Theorem 3. Consider the overall system composed of two leader vehicles (1 and 2) describing a straight-line motion with constant velocity $v_f > 0$. Suppose that ψ_f is known and that vehicle 0 lies in a small neighborhood of the desired position x_d. Then, for appropriately chosen gains K_i and K_p^s, control laws (3.4) (3.7) stabilize ϵ and δ to the origin $\epsilon = \delta = 0$.

Proof. (Theorem 3) Define $\mathbf{x} = \begin{bmatrix} \epsilon & \tilde{v} & \delta \end{bmatrix}^T$ and let $\dot{\mathbf{x}} = f(\mathbf{x})$ be the dynamic equations of (3.2), (3.3) in closed loop with (3.4), (3.7). Further let $\dot{\mathbf{x}} = f^*(\mathbf{x})$ be the simplified dynamics (3.5), (3.8), also in closed loop. We first show that the equilibrium point $\mathbf{x} = 0$ is locally exponentially stable. To this effect, we consider the Lyapunov function

$$V = \mathbf{x}^T P \mathbf{x},$$

with

$$P = \begin{bmatrix} \dfrac{(K_i + \cos \beta^*)\sec^2 \beta^*}{2K_p} & \dfrac{1}{2}\sec \beta^* & 0 \\ \dfrac{1}{2}\sec \beta^* & \dfrac{1 + K_p^2 + K_i \sec \beta^*}{2K_i K_p} & 0 \\ 0 & 0 & \dfrac{1}{2} \end{bmatrix}.$$

Computing its time derivative along the trajectories $\dot{\mathbf{x}} = f^*(\mathbf{x})$ yields

$$\dot{V} \leq a_\epsilon \epsilon^2 + a_{\tilde{v}} \tilde{v}^2 + a_\delta \delta$$

where

$$a_\epsilon = -\rho + \frac{1}{2}(1 - \rho)\left(K_p^s + \frac{1}{K_p^s} + \frac{K_i}{K_p^s}\sec \beta^* \right)$$
$$a_{\tilde{v}} = -K_i \sec \beta^* (1 - \rho) + a_\epsilon$$
$$a_\delta = 2v_f \sin \beta \left(\sin \varphi - \sin(\varphi - \gamma(K_p^h \delta)) \right)$$

and $\rho = \cos \beta \sec \beta^*$ is viewed as an external signal. It can be shown from the definition of ρ and β that, if ϵ is restricted to a bounded region $|\epsilon| < \frac{d}{2} - \mu, \mu > 0$ and appropriate values of K_p^s and K_i are chosen, there exist positive constants q_{11}, q_{22} and q_{33} such that $q_{11} \leq -a_\epsilon$, $q_{22} \leq -a_{\tilde{v}}$ and $q_{33}|\delta| \leq -a_\delta \delta$. This, in turn, yields

$$\dot{V} \leq -\mathbf{x}^T Q \mathbf{x} < 0,$$

with $Q = \mathrm{diag}(q_{11}, q_{22}, q_{33})$ positive definite, guaranteeing local exponential stability. For the second step, we are now interested in the full dynamics, and therefore we introduce

$$\tilde{f}(\mathbf{x}) = f(\mathbf{x}) - f^*(\mathbf{x})$$
$$= \begin{bmatrix} \cos \beta (v_f(\cos \varphi - 1) - v(\cos(\varphi - \gamma(K_p^h \delta)) - 1)) \\ 0 \\ 2\sin \beta (v_f - v)\sin(\varphi - \gamma(K_p^h \delta)) \end{bmatrix}.$$

In this case, $\dot{\mathbf{x}} = f^*(\mathbf{x}) + \tilde{f}(\mathbf{x})$. Using the same Lyapunov function V, we obtain

$$\dot{V} \leq -\mathbf{x}^T Q \mathbf{x} + 2\mathbf{x}^T P \tilde{f}(\mathbf{x}).$$

From the fact that for every small $\eta > 0$, there exists $r > 0$ such that

$$\|\tilde{f}(\mathbf{x})\| < \eta \|\mathbf{x}\|, \quad \forall_{\|\mathbf{x}\| < r},$$

it follows that

$$\dot{V} \leq - \left(\lambda_{min}(Q) - 2\eta \lambda_{max}(P) \right) \|\mathbf{x}\|^2.$$

Choosing a small enough η guarantees that $\dot{V}$ is negative definite in a neighborhood of the origin. $\qquad\square$

3.5 Formation heading estimation

While the control law (3.7) has no dependency on the speed of the leading vehicles, it does depend on the formation heading. The availability of heading information is a reasonable assumption under many scenarios because the acoustic devices used to measure ranges can often transmit additional information, albeit at low data rate. Nevertheless, it restricts the generality and applicability of the approach. In order to eliminate this dependence, we can estimate the formation heading from the observed distances. Replacing α_i into (3.1), we obtain two different estimates for ψ_f:

$$\psi_f^1 = \arcsin\left(\frac{v_1}{v}\sin(\theta_1) - \frac{\dot{z}_1}{v} \right) - \theta_1 + \psi$$
$$\psi_f^2 = \arcsin\left(-\frac{v_2}{v}\sin(\theta_2) + \frac{\dot{z}_2}{v} \right) + \theta_2 + \psi.$$

The exact values of $\dot{z}_i$ are not known, but can be estimated from the evolution of z_i, using e.g. a Kalman filter for the model

$$\dot{\zeta}_{i1} = \zeta_{i2}$$
$$\dot{\zeta}_{i2} = w_i$$
$$\hat{z}_i = \zeta_{i1} + n_i,$$

where w_i and n_i denote process and measurement noise, respectively. In this case, either the following estimates for ψ_f

$$\hat{\psi}_f^1 = \arcsin\left(\frac{\xi}{v}\sin(\theta_1) - \frac{\dot{\hat{z}}_1}{v}\right) - \theta_1 + \psi$$

$$\hat{\psi}_f^2 = \arcsin\left(-\frac{\xi}{v}\sin(\theta_2) + \frac{\dot{\hat{z}}_2}{v}\right) + \theta_2 + \psi$$

or the circular mean

$$\hat{\psi}_f = \arg\left(\frac{1}{2}(\exp(i \cdot \hat{\psi}_f^1) + \exp(i \cdot \hat{\psi}_f^2))\right)$$

can be used to obtain the following result.

Theorem 4. Consider the conditions in Theorem 1 and suppose that $\ddot{z}_i(t)$ and the noises $w_i(t)$ and $n_i(t)$ are bounded signals. Then, the estimation error $\tilde{\psi}_f = \hat{\psi}_f - \psi_f$ converges to a small neighborhood of zero. More precisely, there exist positive constants $c_i, i = 1, 2, 3$ such that

$$\lim_{t\to\infty}\sup|\tilde{\psi}(t)| \le \sum_{i=1}^2\left(c_1\lim_{t\to\infty}\sup|w_i(t)|\right.$$
$$\left. + c_2\lim_{t\to\infty}\sup|n_i(t)| + c_3\lim_{t\to\infty}\sup|\ddot{z}_i(t)|\right).$$

4. EXTENSION TO MARINE VEHICLES

This section indicates how the results derived can be applied to autonomous marine vehicles. To this effect, we adopt the model of the MEDUSA class of autonomous semi-submerged robotic vehicles developed at the Laboratory of Robotics and Systems in Engineering and Science (LARSyS), Instituto Superior Técnico, shown in Fig. 4.1.

Each Medusa weighs approximately $30\,\mathrm{Kg}$ and consists of two stacked longitudinal acrylic housings, with a total length of around $1\,\mathrm{m}$. It carries a standard EPIC single-board computer, a combined inertial measurement unit and attitude heading reference system, a GPS receiver and an underwater camera. A long-range 802.11 interface is used for surface communications, while an acoustic modem enables underwater communication. The vehicle is propelled by two side-mounted, forward-facing stern thrusters that directly control surge and yaw motion.

Since the vehicle only operates on the horizontal plane, its kinematics equations take the simple form

$$\dot{x} = u\cos\psi - v\sin\psi \qquad (4.1)$$
$$\dot{y} = u\sin\psi + v\cos\psi$$
$$\dot{\psi} = r,$$

where u (surge speed) and v (sway speed) are the body axis components of the velocity of the vehicle, x and y are the Cartesian coordinates of its center of mass, ψ defines its orientation (heading angle), and r its angular velocity. Under an unperturbed straight-line motion, $r = v = 0$ and (4.1) reduces to our simple kinematic model (2.1).

The motions in heave, roll and pitch can be neglected, as the vehicle is a surface craft with large enough metacentric height. The resulting simplified dynamic equations of motion for surge, sway and yaw are

$$m_u\dot{u} - m_v vr + d_u u = \tau_u$$
$$m_v\dot{v} + m_u ur + d_v v = 0$$
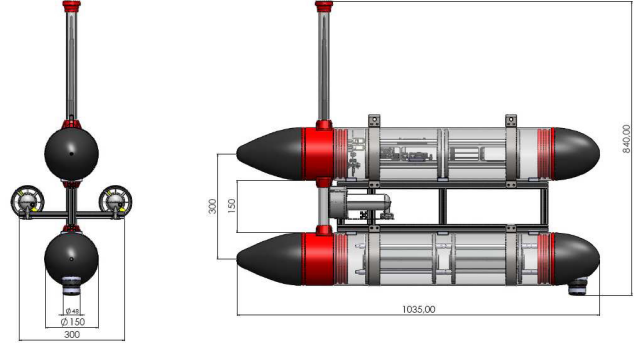$$m_r\dot{r} - m_{uv}uv + d_r r = \tau_r,$$

Fig. 4.1. Front and side view of the Medusa AMV

where τ_u stands for the external force in surge (thruster common mode), τ_r for the external torque (thruster differential mode), the m terms represent vehicle masses and hydrodynamic added masses, and the d terms are functions of the velocity and represent hydrodynamic damping effects. The thruster model includes a first order system $K_0/(s + K_0)$, with $K_0 = 7.2115$ and an additional delay of $0.346\,\mathrm{s}$. The full set of Medusa physical parameters can be found in Ribeiro et al. (2012).

We consider the practical situation in which there exist inner-loop controllers designed to track reference signals in u and ψ. These autopilot controllers are also detailed in Ribeiro et al. (2012).

This model has been used for simulations and hardware-in-the-loop testing, and has been fitted with extensive experimental data, providing an accurate representation of the real dynamics of the vehicle. While the current vehicle is restricted to surface operations, the proposed motion control algorithms hold for the future envisioned scenario of constant-depth underwater operations supported by surface vehicles.

5. SIMULATION RESULTS

Simulations were run using MATLAB with the complete model of the Medusa. The leading vehicles follow a predetermined lawnmower path with $v_f = 0.2 m/s$. The paths of the leading vehicles (gray) and of the follower (black) are presented in Fig. 5.1.

Fig. 5.2 shows the common and differential mode errors. Both tend towards 0 in steady state although, turns are accompanied by some additional error. Note, however, that common-mode error stays below $0.2\,\mathrm{m}$, and differential mode error never goes over $0.5\,\mathrm{m}$. The heading estimation error, $\tilde{\psi}$, is also shown. While turning, $v_1 \ne v_2 \ne v$, deteriorating the estimate $\hat{\psi}$. Even so, it tracks the formation heading with a maximum error under $30\,^\circ$.

The speed and heading evolution are shown in Fig. 5, versus the formation parameters. The vehicle heading displays some overshoot, but quickly tends to zero error when in straight-line movement, where all simplifying assumptions are valid. The speed controller exhibits a slight oscillation, even in straight line. This oscillation is mostly due to the complex dynamics involved, with significant command delays, and does not occur when using simplified dynamics.
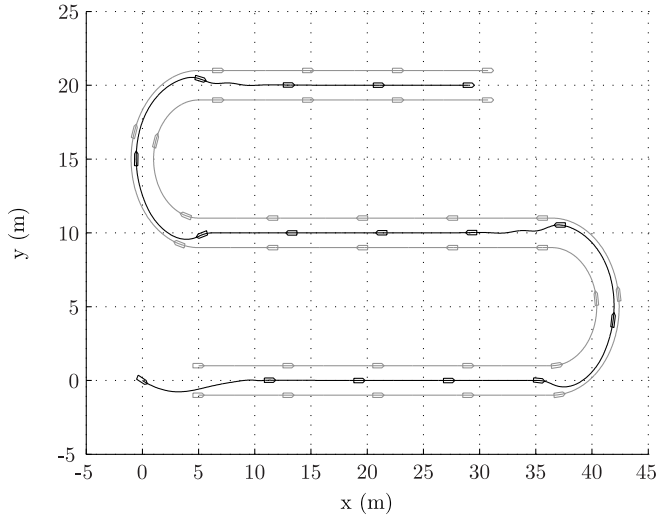
Fig. 5.1. Vehicle Paths. The maneuver starts on the lower left corner. The leader vehicles and the follower vehicle are shown in light and dark colours, respectively.
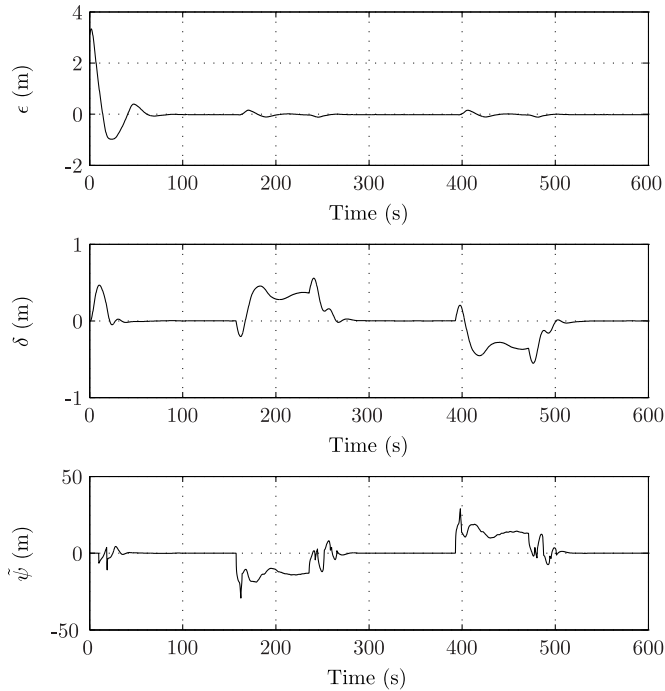

Fig. 5.2. Time evolution of the common mode, differential mode, and heading estimation error ϵ

6. CONCLUDING REMARKS

This paper advanced a solution to a three-vehicle formation keeping problem where a follower moves in a triangular formation behind two leading vehicles, using only inter-vehicle range measurements and with no knowledge of the path taken by the leaders.

Proofs of error convergence were presented for a straight-line motion, and preliminary simulation results were described for a lawnmower motion, using the dynamics of a real marine vehicle.

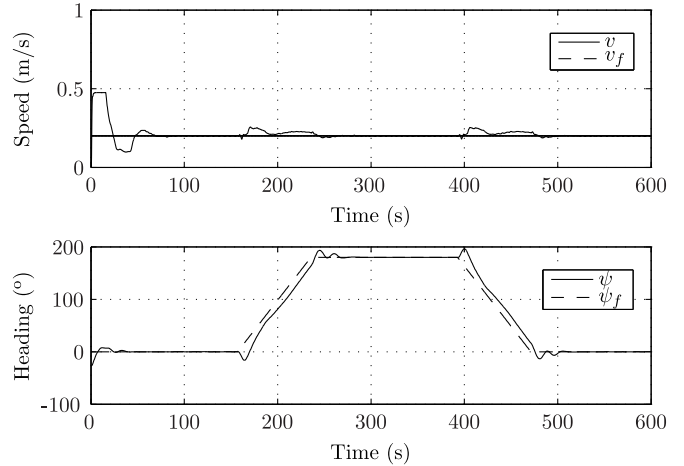The next step in the development of this approach will be to extend the algorithm to deal with more realistic

Fig. 5.3. Time evolution of the vehicle and formation speeds v and v_f, and headings ψ and ψ_f

conditions where range measurements are only available at discrete points in time, usually with a period of several seconds, and subjected to sensor noise and outliers, as well as frequent communication delays and temporary losses. Future work will address the implementation and testing of selected algorithms in real marine scenarios using the Medusa vehicles developed at the ISR/IST.

REFERENCES

Cao, M. and Morse, A.S. (2007). Station keeping in the plane with range-only measurements. In *2007 American Control Conference*, 5419–5424. IEEE, New York, NY, USA. doi:10.1109/ACC.2007.4282748.

Cao, M. and Morse, A.S. (2008). The use of dwell-time switching to maintain a formation with only range sensing. In *Communications, Control and Signal Processing, 2008. ISCCSP 2008. 3rd International Symposium on*, March, 954–959. IEEE, St. Julians, Malta.

Cao, M., Morse, A.S., Yu, C., Anderson, B.D.O., and Dasguvta, S. (2007). Controlling a triangular formation of mobile autonomous agents. In *2007 46th IEEE Conference on Decision and Control*, 3603–3608. IEEE. doi:10.1109/CDC.2007.4434757.

Cao, M., Yu, C., and Anderson, B.D.O. (2011). Formation control using range-only measurements. *Automatica*, 47(4), 776–781. doi:10.1016/j.automatica.2011.01.067.

Desai, J., Ostrowski, J., and Kumar, V. (1998). Controlling formations of multiple mobile robots. In *Robotics and Automation, 1998. Proceedings. 1998 IEEE International Conference on*, volume 4, 2864–2869. IEEE, Leuven, Belgium. doi:10.1109/ROBOT.1998.680621.

Desai, J., Ostrowski, J., and Kumar, V. (2001). Modeling and control of formations of nonholonomic mobile robots. *Robotics and Automation, IEEE Transactions on*, 17(6), 905–908. doi:10.1109/70.976023.

Ghabcheloo, R., Aguiar, A.P., Pascoal, A.M., Silvestre, C., Kaminer, I., and Hespanha, J. (2009). Coordinated path-following in the presence of communication losses and time delays. *SIAM Journal on Control and Optimization*, 48(1), 234. doi:10.1137/060678993.

Ribeiro, J., Aguiar, A.P., and Pascoal, A.M. (2012). Motion control design for the Medusa robotic vehicle with experimental results. Technical report, LARSyS, Lisbon, Portugal.